

The Structure of p-Aminobenzoic Acid in Water: Studies Combining UV-Vis, NEXAFS and RIXS Spectroscopies

This content has been downloaded from IOPscience. Please scroll down to see the full text.

2016 J. Phys.: Conf. Ser. 712 012034

(<http://iopscience.iop.org/1742-6596/712/1/012034>)

View [the table of contents for this issue](#), or go to the [journal homepage](#) for more

Download details:

IP Address: 129.11.22.158

This content was downloaded on 11/07/2016 at 14:38

Please note that [terms and conditions apply](#).

The Structure of *p*-Aminobenzoic Acid in Water: Studies Combining UV-Vis, NEXAFS and RIXS Spectroscopies

A Gainar¹, J S Stevens¹, E Suljoti², J Xiao², R Golnak², E F Aziz^{2,3}, S L M Schroeder^{1,4,5}

¹School of Chemical Engineering and Analytical Science, The University of Manchester, Oxford Road, Manchester, M13 9PL, UK

²Joint Ultrafast Dynamics Lab in Solutions and at Interfaces (JULiQ), Helmholtz-Zentrum Berlin für Materialien und Energie Institution Albert Einstein Strasse 15, 12489 Berlin, Germany

³Freie Universität Berlin, Arnimallee 14, 14195 Berlin, Germany

⁴School of Chemical and Process Engineering, University of Leeds, Leeds, LS2 9JT, UK

⁵DIAMOND Light Source Ltd, Chilton, Didcot, OX11 0QX, UK

E-mail: ¹adrian.gainar@postgrad.manchester.ac.uk; ^{1,4,5}s.l.m.schroeder@leeds.ac.uk

Abstract. NEXAFS-RIXS and home laboratory-based UV-Vis absorption spectroscopy are combined to examine the speciation and electronic structure of *para*-aminobenzoic acid (PABA) in aqueous solution as a function of pH. DFT and TD-DFT electronic structure calculations reproduce the experimental trends and provide a correlation between the experimental HOMO↔LUMO gap as well as the electronic transitions between molecular orbitals in the non-ionic, anionic and cationic forms of PABA.

1. Introduction

Para-aminobenzoic acid (PABA) has therapeutic effects and sunscreen properties due to its capability to filtering out UV radiation through the electronic conjugation of the *para* orientated amino and carboxyl substituents through the aromatic ring. Core-level spectroscopies such as near-edge X-ray absorption fine structure (NEXAFS) and resonant inelastic X-ray scattering (RIXS) have given incisive insight on the electronic state of PABA species in solution and in the solid state including the anionic and cationic forms in water [1]. While NEXAFS involves excitation of electrons from 1s core orbitals to unoccupied molecular orbital (MO) levels (*e.g.* lowest unoccupied MO, LUMO), RIXS probes transitions from occupied MOs (*e.g.* highest occupied MO, HOMO) to 1s core orbitals. UV-Vis spectroscopy is quite similar to these core level techniques in that it probes electronic transitions, but from occupied MOs such as σ , n (non-participant) or π type orbitals to σ^* or π^* unoccupied MOs. As NEXAFS, RIXS and UV-Vis often probe the same final-state MOs, their combined measurement supported by electronic structure calculations (particularly density functional theory, DFT, and time-dependent density functional theory, TD-DFT) provides an opportunity to arrive at a deeper understanding of the local electronic structure landscape.



2. Experimental

2.1. Materials

PABA crystalline powder (99%, Sigma-Aldrich, UK) was dissolved in distilled, deionized water. pH of the solution was adjusted by dropwise addition of 1.2 M aqueous solution of NaOH or of HCl.

2.2. Transmission UV-Vis

A saturated stock solution of 0.03 M PABA in water was prepared and successively diluted to reach the detection range of the Beckman DU 520 spectrophotometer.

2.3. Gaussian calculations

Non-ionic, anionic and cationic PABA monomers were ground-state optimized with B3LYP/6-31G* in Gaussian09 to obtain the DFT molecular orbitals. Using these optimized monomers in a water continuum, TD-DFT polarizable continuum model (PCM) calculations were employed to generate the simulated spectra and the MOs involved in these transitions.

2.4. NEXAFS/RIXS

NEXAFS and RIXS were recorded at the N K-edge (resolution ≤ 0.1 eV) using the liquid microjet of the LiXEdrom endstation, U41-PGM beamline, BESSY II synchrotron. The common energy scale was calibrated using N₂ gas, measuring the 1s \rightarrow 2p π transitions in total electron yield mode.

3. Results and discussion

Depending on the pH of the aqueous solution, PABA is present in cationic, neutral or anionic form [1,2]. For low (acidic) pH solution (where PABA is almost entirely present as the cationic species), the main absorption band is centered at a wavelength of ~ 225 nm. For high pH, PABA is anionic and the main UV absorption peak occurs at ~ 265 nm, while the neutral species, at intermediate pH, absorbs at ~ 275 nm (Table 1 and Figure 1). TD-DFT calculations reproduce the observed trend, with the main absorption shifted to shorter wavelengths compared to non-ionic PABA (cationic < anionic < non-ionic, Table 1). Within this trend, it is noticeable that the calculated value for the anionic species is significantly lower than the experimentally observed value. It has been suggested previously that calculated charge transfer excitations can be less accurate for ionic π systems due to underestimated excitation energies of ionic components [3]. Perhaps it also plays a role here that the carboxylate group is less electron withdrawing and thus electrons are more consolidated around this group rather than being delocalized over the ring [4].

Table 1. Comparison of main absorption wavelengths in experimental UV-Vis and TD-DFT simulated spectra of PABA species in water, with primary transitions from HOMOs to LUMOs.

PABA species	Wavelength (experimental) / nm	Wavelength (simulated) / nm	Primary transition
Non-ionic	~ 275	266.96	HOMO \rightarrow LUMO
Anionic	~ 265	228.26	HOMO-1 \rightarrow LUMO
Cationic	~ 225	218.95	HOMO-1 \rightarrow LUMO

Collating together the snapshots of the MOs generated from the TD-DFT calculations for the non-ionic, anionic and cationic monomers in water, Figure 1 reveals that the primary transition in the non-ionic PABA takes place between the orbital with annotation A as HOMO and the $1\pi^*$ orbital as LUMO (~ 267 nm, 4.64 eV), whereas the shift to shorter wavelength in the anionic PABA is due to widening energy separation between A and $1\pi^*$ (~ 228 nm, 5.43 eV), with A lowering in energy and becoming HOMO-1. Similarly, the noted shift to lower wavelength for cationic PABA (~ 219 nm, 5.66 eV) can be explained by the primary transition between A, which is now the HOMO-1, and $1\pi^*$.

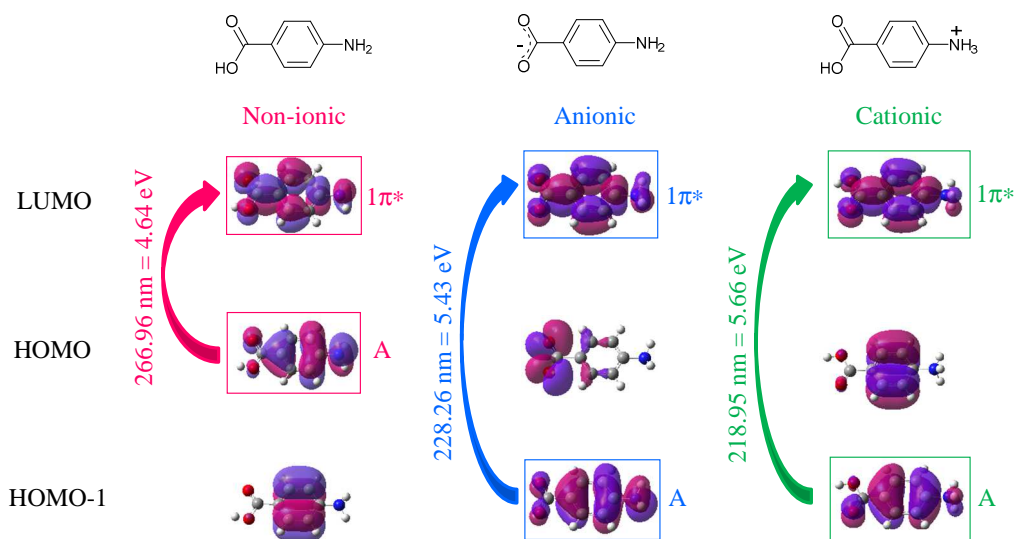


Figure 1. Transitions (arrows) between MOs of interest A and $1\pi^*$ (marked with boxes) in TD-DFT calculations for non-ionic, anionic and cationic PABA monomers in a water continuum.

We can now correlate these observations with the MO information for these systems that we have previously obtained by RIXS and NEXAFS [1]. Figure 2 shows that the experimentally determined HOMO \leftrightarrow LUMO gap for nitrogen (which is not applicable to cationic PABA due to the protonation of nitrogen) is correlated with the calculated energy gap between orbitals A and $1\pi^*$ from the DFT calculations for the non-ionic and anionic species. In the case of non-ionic PABA, orbital A corresponds to the HOMO and orbital $1\pi^*$ to the LUMO, whilst for the anionic species, orbital A lowers down in energy becoming HOMO-3 and orbital $1\pi^*$ raises up in energy as LUMO+1.

Although core hole relaxation effects are expected to affect the energetic position of features in the NEXAFS and RIXS data, the impact on taking the experimental RIXS-NEXAFS energy gap as a measure of the HOMO-LUMO is believed to be of the order of at most a few 100 meV; additionally, when such effects were included in CASTEP calculations for crystalline PABA [5] the inclusion of final-state effects did not change the MO interpretation significantly. For the DFT calculations, omitting relaxation effects may lead to a slight overestimation of transition energies, and thus of the RIXS-NEXAFS energy gap. The reason for the weak effects of relaxation are the strong localized core-level excitations and the weak nature of the intermolecular interactions (*i.e.* hydrogen bonding) compared to intramolecular interactions (*i.e.* covalent bonds and protonation effects).

Table 2. Values for the energy gap of interest A \leftrightarrow $1\pi^*$ reflected by the experimental UV-Vis, RIXS-NEXAFS, and by TD-DFT and DFT calculations.

Energy gap A \leftrightarrow $1\pi^*$	Non-ionic PABA	Anionic PABA
UV-Vis (experimental)	~ 4.51 eV	~ 4.68 eV
TD-DFT (calculated)	4.64 eV	5.43 eV
RIXS-NEXAFS (experimental)	5.06 eV	5.89 eV
DFT (calculated)	5.01 eV	5.86 eV

The differences noted in the A \leftrightarrow $1\pi^*$ gap presented in Table 2 between UV-Vis and RIXS-NEXAFS spectroscopies may be explained through the presence of a hole in the valence band in the UV-Vis, that exerts a smaller effect over the final state than the core hole from RIXS-NEXAFS. The TD-DFT PCM calculations also involve a water continuum (thus PABA surface-polarized monomers

with slightly different MO energy levels), yet this rather simplistic model is sufficient to picture the increase of the $A \leftrightarrow 1\pi^*$ energy gap when moving from non-ionic to anionic PABA species.

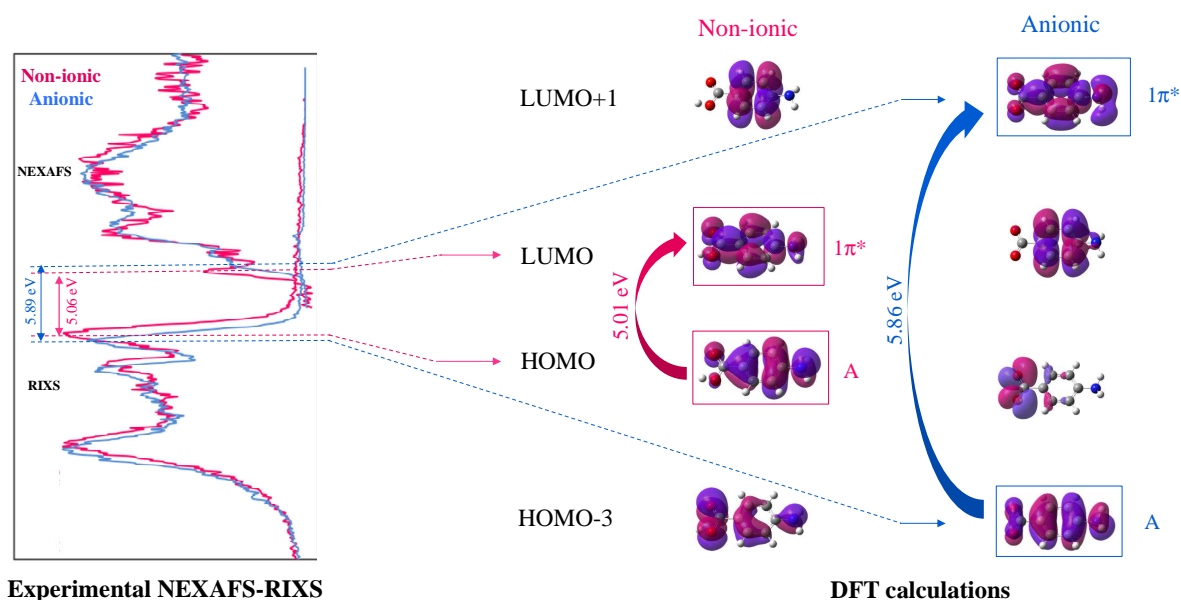


Figure 2. Nitrogen RIXS and NEXAFS showing the $HOMO \leftrightarrow LUMO$ gap for non-ionic and anionic species, correlated with transitions (arrows) between DFT MOs of interest labelled as A and $1\pi^*$.

4. Conclusions

Monitoring the electronic transitions of PABA in the UV range in aqueous solution at intermediate, high and low pH, and interpreting the results with TD-DFT calculations provides a spectroscopic identification of PABA species that is complementary to the fine detail arising from the previously reported NEXAFS-RIXS combination. The effect of pH can be translated in the UV-Vis by the shifts to shorter wavelengths in the main absorption peaks encountered in the spectra of high and low pH solutions with respect to the intermediate pH solutions, which are reflected by the TD-DFT simulations. These shifts are explained by $A \leftrightarrow 1\pi^*$ energy gap alterations with the changes in electronic structure accompanying the pH variation; the DFT calculations associated with the experimental RIXS-NEXAFS identify well with the orbital gap observed in the TD-DFT simulations that reflects the main absorption peaks in the UV-Vis, thus bridging the synchrotron X-ray core-level spectroscopies NEXAFS and RIXS with the laboratory UV-Vis technique.

Acknowledgements

This work was supported by the EPSRC Critical Mass Grant EP/I013563/1 and use of synchrotron at BESSY II (HZB) by European Community's Seventh Framework Programme, grant no. 312284.

References

- [1] Stevens J S, Gainar A, Suljoti E, Xiao J, Gohnak R, Aziz E F and Schroeder S L M 2015 *Chem. Eur. J.* **21** 7256–63.
- [2] van de Graaf B, Hoefnagel A J and Wepster B M 1981 *J. Org. Chem.* **46** 653–57.
- [3] Grimme S and Parac M 2003 *Chem. Phys. Chem.* **3** 292-95.
- [4] Lampman G M, Pavia D L, Kriz G S and Vyvyan J R 2001 *Spectroscopy* (Belmont: Brooks/Cole Cengage Learning).
- [5] Stevens J S, Seabourne C R, Jaye C, Fischer D A, Scott A J and Schroeder S L M 2014 *J. Phys. Chem. B* **118** 12121–28.